



Investigation of Site Characterization in the Akdeniz Region by Using Seismic Refraction and Surface Wave Methods

Cengiz Kurtuluş*

Department of Geophysics,
Kocaeli University, Kocaeli, Turkey

Hamdullah Livaoglu

Department of Geophysics,
Kocaeli University, Kocaeli, Turkey

Fadime Sertçelik

Department of Geophysics,
Kocaeli University, Kocaeli, Turkey

İbrahim Sertçelik

Department of Geophysics,
Kocaeli University, Kocaeli, Turkey

Sena İblikçi

Department of Geophysics,
Kocaeli University, Kocaeli, Turkey

Abstract: Multichannel Analysis of Surface Waves (MASW), Refraction Microtremor (ReMi), and Microtremor measurements was performed to predict site characterization at 65 strong-motion stations of AFAD (Disaster and Emergency Management Presidency) in the Akdeniz region in Turkey. Reliable field response information is required to investigate the region's impacts and assess the risk of the area. The soil conditions of the Akdeniz region are specified from MASW, ReMi, and Microtremor studies of AFAD's strong motion stations in this area. HVSR technique was conducted to determine dominant frequency values at different amplification levels. The Akdeniz region was classified according to V_{S30} based NEHRP Provisions [1], Eurocode-8 [2] and TBDY-2018 [3] and Rodrigez-Marek [4]. According to the [1], one station is classified as class A, 7 stations as B and 38 stations as C and 19 stations to be class D. According to [2], 6 stations correspond to class A, 39 stations B, and 20 stations D. The soil classes in the NEHRP system correspond to that of TBDY-2018 [3]. According to [4], 8 stations are classified as A, 17 stations B, 8 stations C-1, 13 stations C-2, 5 stations C-3, 11 stations D-1, 1 station D-2, 1 station D-3, 1 station E and 1 station is undistinguished. The predominant period of the region ranges from 0.07 to 1.47s, and the dominant magnification values vary between 0.79 and 8.5.

Keywords: MASW, ReMi, microtremor measurements, Akdeniz region, Turkey

Received: 17 July 2018; **Accepted:** 18 September 2018; **Published:** 14 November 2018

I. INTRODUCTION

The Akdeniz (Mediterranean) region is located in a seismically active region in the southern part of Turkey. It constitutes about 15% of the total area of Turkey with a surface area of approximately 120,000 km². The tectonic activity of the region shows a complex tectonic behavior under the influence of the faults of the Dead Sea, Eastern Anatolia and Cyprus [5]. In the last century (BC 37-2015),

the ten largest destructive earthquakes in this area have shown that local site conditions have a major impact on the ground shaking. It has been reported that the tsunamis occurring in 1822 and 1872 earthquakes in Hatay lead to the death of 20 thousand people [6]. Microtremor survey of the various regions in Turkey, earthquake monitoring, a surface wave of research and several field effect study about the drilling data have been conducted [7, 8,

*Correspondence concerning this article should be addressed to Cengiz Kurtuluş, Department of Geophysics, Kocaeli University, Kocaeli, Turkey. E-mail: cengizk52@gmail.com

9, 10, 11, 12, 13, 14, 15, 16, 17, 18, 19, 20, 21, 22, 23]. [13] have used (H/V) spectral ratios to predict the strong motion site condition of Turkey. [15] and [24] applied geophysical and geotechnical studies in order to determine the field classification of Turkish strong movement areas. [25] analyzed the microtremor data for Antakya and suggested the initial micro-zonation map proposed for Antakya province based on the dominant periods ranging from 0.2 to 0.8 sec and the shear wave velocities of the sediments covering the region. [26] examined the relationship between ground conditions and earthquake effect in Antakya. [27] investigated the seismicity of the region between Adana and Antakya-Kahramanmaraş with b and

risk analysis. [28] attempted to investigate the local site effects of MATNet, which consists of 55 uniaxial force balance accelerometers, and tried to record explosions that could be established near Hatay-K.Maras sites and evaluate them as part of an early warning and pre-damage estimate system. [29, 30] conducted microtremor array research on shallow S wavelength velocity profiles in 41 sites in the Akdeniz region. In this study, seismic refraction, MASW, refraction microtremor (ReMi) and microtremor studies were carried out to investigate the distribution of S-wave velocity in shallow soils at 65 strong motion stations in Akdeniz region (Figure 1).

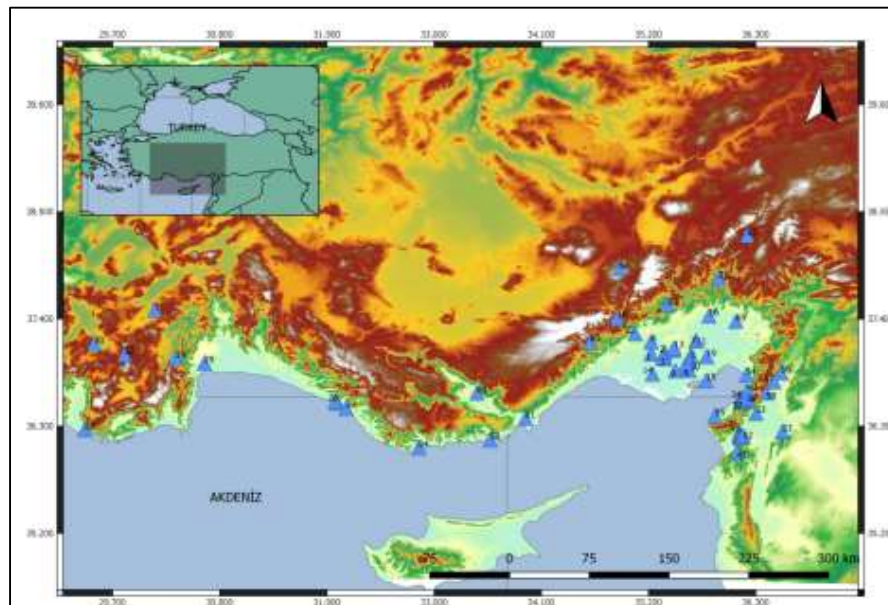


Fig. 1. Location of the study area. Triangles indicate the measuring stations

II. GEOLOGY AND TECTONICS OF THE REGION

The Miocene aged Neritic limestones are generally found in the Hatay region. Miocene aged carbonate and clastics are formed in the east of the region. Ordovician aged carbonates, Jura Neritic limestone, low-middle Cambrian quartz, Quaternary limestone are located in the central coastal areas. The Amanos Mountains and the Kzldag ophiolite massif at the south end of the Eastern Taurus Mountains also have an important place in the geology of the region (Figure 2). Pleistocene undifferentiated clastic are generally located in Adana and Hatay

regions. Most of the mountains in the Mediterranean region constitute the western and central Taurus. Amanos Mountains and Samandag are among the important mountains in the east of the region. The Mediterranean region and its surrounding seismicity were formed as a result of the African and Arabian plates moving northwardly according to Eurasia. The African plate has been moving northward at about 10 mm per year in relation to Eurasia [31, 32]. Deep structures in the region, generally E-W-oriented slope-displacement normal faults, north-south-oriented strike-slip faulting, and west of the study area again consists of graben-horst block systems developing this tectonic result.

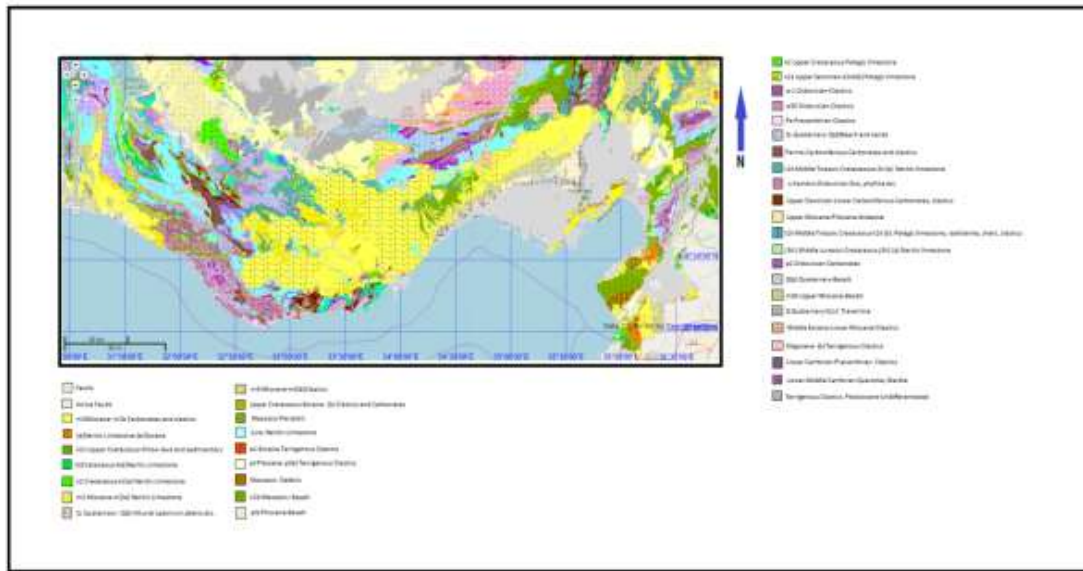


Fig. 2. Geological map of Akdeniz region

III. DATA ACQUISITION AND ANALYSIS

Seismic refraction, MASW, REMI, and microtremor data were collected at AFAD’s 65 strong motion stations in Akdeniz region, southern Turkey.

Seismic refraction data were recorded for 2 sec with a sampling rate of 1 msec using a 50kg weight dropper energy source 48 4.5 Hz P-wave geophones were fixed at 2m geophone intervals in line (Figure 3).

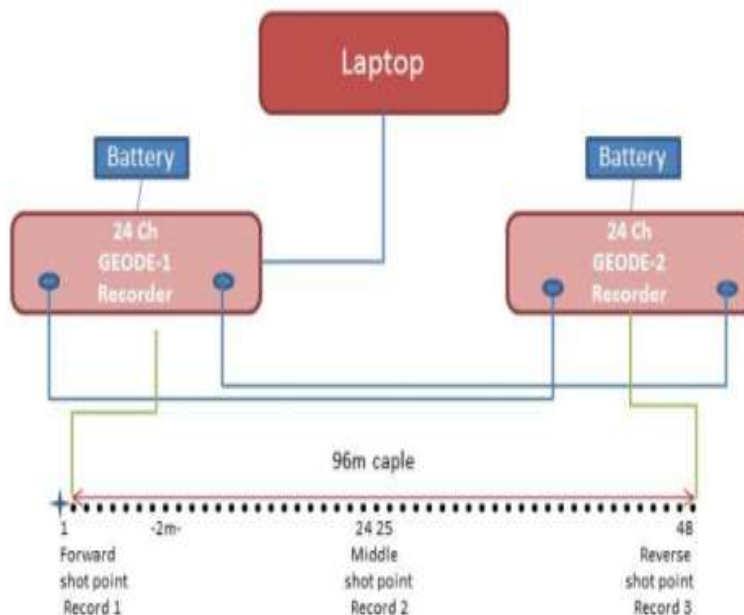


Fig. 3. Schematic of MASW data acquisition with a 48-channel linear receiving array

The shot records at each side were used in the analysis of the surface waves (MASW) to estimate the V_{s30} profiles of the topmost 30m. The shot records were insulated from the refracted and reflected waves by muting at first and afterward. It was filtered 2-4, 36-48 Hz

band-pass filter to remove low and high frequency noise (Figure 5(a)). Later, plane wave decomposition was applied to transform the data from offset time to phase the velocity-against frequency domain [33, 34].

The dispersive curve of the fundamental mode of surface waves are picked from this domain. S-wave velocity as a function of depth was determined to invert the dis-

persion curve. For the fundamental mode, the dispersion curve representing the variation of the phase velocity with respect to frequency is determined as shown.

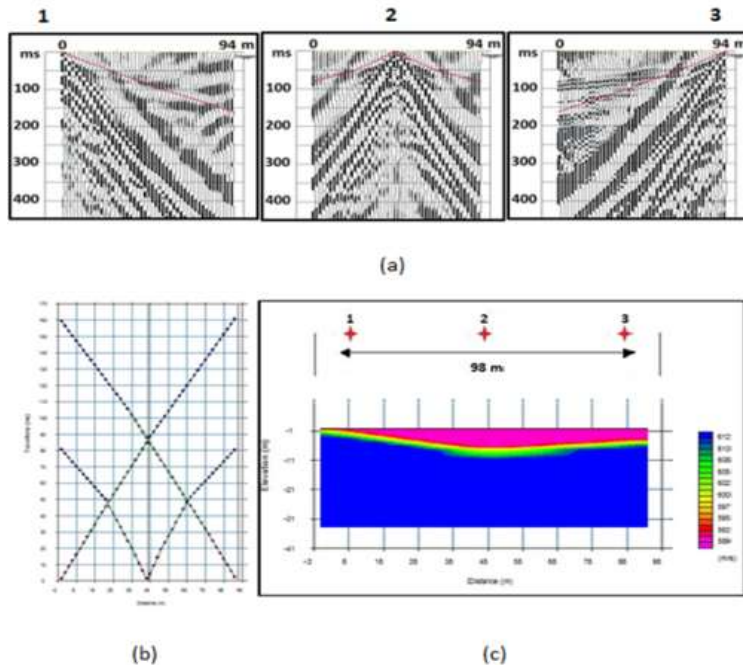


Fig. 4. (a) Seismic refraction records with picked first arrival times showing in red line collected at the station no:0117 (b) travel time curves of mid-point shot, (c) P-wave velocity-depth model

This dispersion curve was used to determine the S-wave velocity-depth profile of the stationary zone and the S-wave velocity-depth profile by the inversion method

(Figure 5(b)). The dispersion curve showing the variation of the frequency and phase velocity for the basic mode is shown in Figure 5(c).

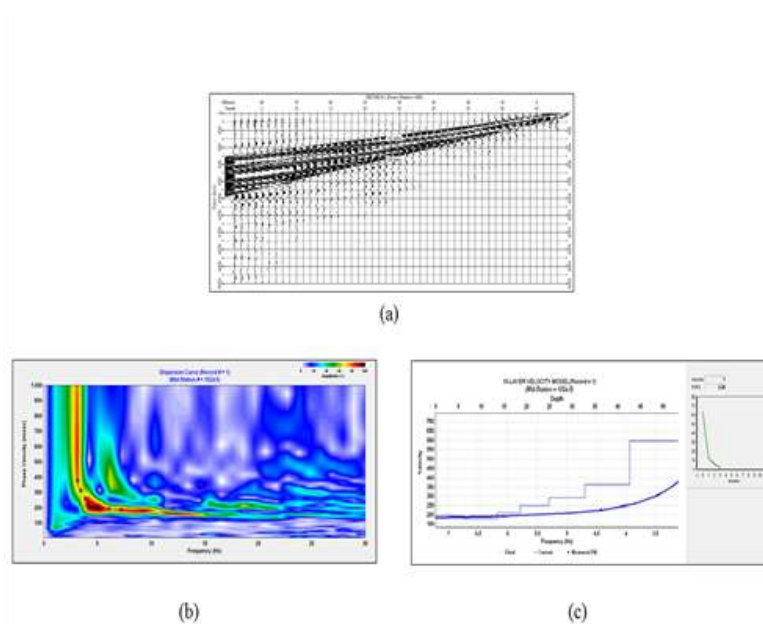


Fig. 5. (a) the shot record separated from the refraction and reflected waves at 0117 coded stations, (b) MASW dispersion spectrum of the surface waves. The MASW S-wave-depth profile (blue) and the modeled dispersion curve (black), (c) Vs-depth profile and modeled dispersion curve.

The ReMi data were recorded as 32 seconds with a sampling rate of 2 sec with the same field pattern as the seismic source, usually using ambient noise from the wind and traffic. 24-25 records are stacked in each ReMi installation. Rayleigh waves are distinguished from other waves using two-dimensional slowness frequencies (p-f) transforms of noise recordings in both directions. The Rayleigh wave dispersion is selected along the minimum velocity envelope of the energy in the slowness frequency spectral image. These Rayleigh wave dis-

ersion curves are modeled by using the velocity-depth model to determine the shear wave velocity depth profile. The time-distance data are shown in Figure 6(a). The dispersive curve of the basic mode of surface waves is taken from this domain. S-wave velocity as a function of depth was determined inverting the dispersion curve (Figure 6(b)). This dispersion curve was used to determine the S-wave velocity-depth profile of the stationary zone by the inversion method Figure 6(c).

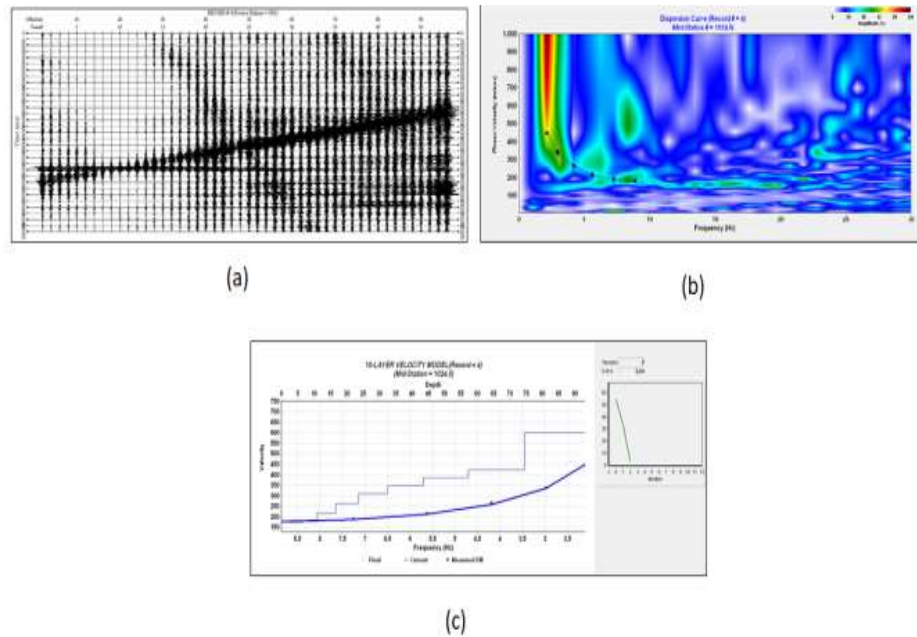


Fig. 6. (a) ReMi data at 0117 coded station, (b) the dispersion spectrum calculated by separating the plane-wave components of the surface waves present in the seismic record, (c) S-wave velocity-depth profile (blue) and modeled dispersion curve (black). The vertical axis indicates the S-wave velocity and the horizontal axis shows the frequency of the dispersion curve.

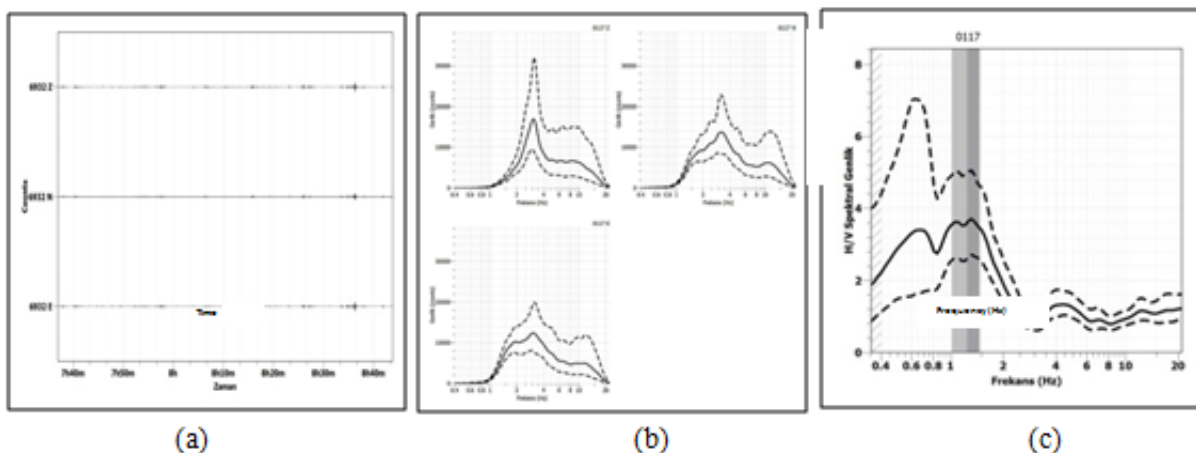


Fig. 7. a) Filtered time signal series, b) The amplitude spectra of the three components microtremor data the peak and (c) the H/V amplitude spectrums. The dashed lines show the standard deviation of amplitude and the two vertical gray areas indicate the peak frequency standard deviation domains.

The velocity-based broadband sensor (0.03-50 Hz straight response) was used for ambient noise recording. Whole data were recorded with the same sensor Figure 7(a) and Figure 7(b). The H/V amplitude spectrum of the dominant frequency and the amplification of the 0117 coded stations is shown in Figure 7(c). As depicted in Figure 7, the microtremor dominant period is 0.80 seconds with 1.125 Hz frequency, and H/V peak amplitude values were 3.6. The predominant period of

the region ranges from 0.07 to 1.47s and the dominant magnification values vary between 0.79 and 8.5.

A. Site Classification for the Investigation Area

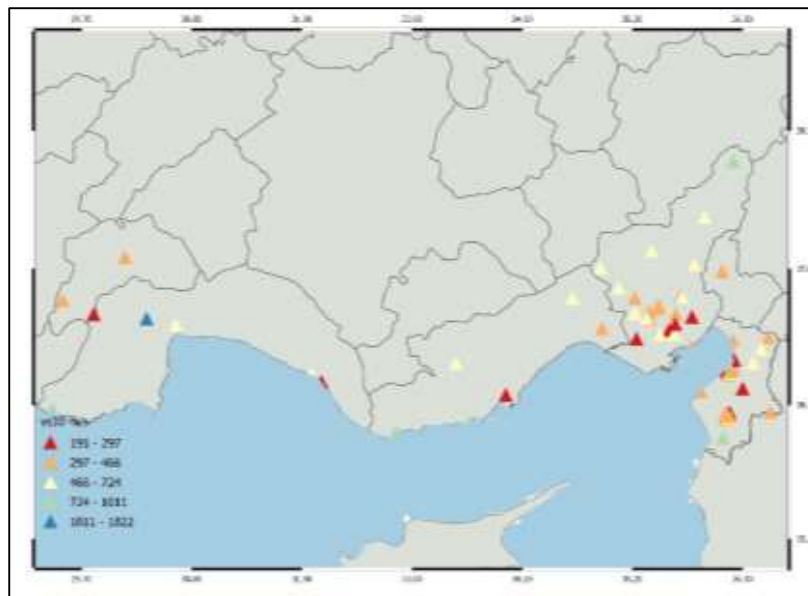
MASW, ReMi, and microtremor methods were conducted at 65 stations and V_{s30} velocity profiles were determined for the uppermost 30 m. The V_{s30} values range from 191 to 1822m/s. The lower velocities are generally determined on the plain areas (Figure 8 and Table 1).

TABLE 1
LIST OF THE CLASSES FOR THE STRONG MOTION STATIONS IN AKDENİZ PROVINCE

Station Code	Station Name	Lat (°N)	Lon (°E)	V_{s30} (m/s)	H/V peak amplitude	Predominant period (sn)	[1]	[2]	[3]	[4]	
1	101	STATION	37,044	35,226	478	3.7	1.47	C	B	ZC	D-3
2	102	STATION	37.05792	35.36698	417	3.05	0.21	C	B	ZC	C-1
3	103	STATION	36.995811	35.3706	423	1.01	0.20	C	B	ZC	C-1
4	106	CEYHAN	36.908	35.567	210	3.15	0.55	D	C	ZD	C-3
5	107	CEYHAN	37.033	35.633	405	3.1	0.67	C	B	ZC	C-3
6	108	CEYHAN	36.876	35.617	654	2.00	0.14	C	B	ZC	C-1
7	109	CEYHAN	37.178	35.689	253	2.7	1.17	D	C	ZD	D-2
8	111	SEYHAN	37.166	35.226	461	0.79	0.43	C	B	ZC	C-2
9	112	YUREGİR	36.871580	35.476279	490	1.6	0.57	C	B	ZC	C-3
10	113	YUREGİR	36.955522	35.627320	267	3.11	0.50	D	C	ZD	C-3
11	114	YUREGİR	37.175843	35.69286	483	1.05	0.66	C	B	ZC	C-3
12	115	YUREGİR	37.081210	35.454380	322	2.1	1.01	D	C	ZD	D-2
13	116	YUREGİR	37.104862	35.462624	466	0.8	0.55	B	C	ZB	C-3
14	117	YUREGİR	36.838383	35.241111	215	3.6	0.80	D	C	ZD	D-2
15	120	YUREGİR	36.77006	35.79005	439	3.1	0.16	C	B	ZC	C-1
16	122	KOZAN	37.4339	35.82021	501	3.1	0.13	C	B	ZC	C-1
17	123	YUREGİR	37.00338	35.34376	519	6.7	0.2	C	B	ZC	C-1
18	124	POZANTI	37.4087	34.87911	583	5.8	0.16	C	B	ZC	C-1
19	125	CEYHAN	37.01519	35.79577	216	1.94	1.03	D	C	ZD	D-2
20	126	ALADAG	37.54551	35.39186	521	2.4	0.22	C	B	ZC	C-1
21	127	FEKE	37.81619	35.92038	583	3.3	0.16	C	B	ZC	B
22	128	KARAIŞALI	37.25029	35.06279	494	2.3	0.8	C	B	ZC	D-1
23	129	TUFANBEYLİ	38.25915	36.21013	965	2.1	0.1	B	A	ZB	B
24	707	KORKUTELİ	37.0007	30.35028	1822	3.8	1.47	A	A	ZA	C-2
25	713	ALANYA	36.54286	32.00434	540	2.4	0.47	C	B	ZC	C-2
26	714	ALANYA	36.55547	31.98667	607	1.4	0.47	C	B	ZC	C-2
27	715	MAHMUT-LAR	36.48778	32.09627	285	4.8	0.8	D	C	ZD	D-2
28	716	KALKAN	36.2685	29.4128	813	<2	0.5-0.1	B	A	ZB	
29	717	KEPEZ	36.9495	30.6419	724	1.7	0.19	C	B	ZC	C-1
30	1506	GOLHİSAR	37.14721	29.50946	337	1.6	0.58	D	C	ZD	C-3
31	1507	KOZLUCA	37.4942	30.1336	359	0.8	1.1	D	C	ZD	C-3
32	1508	SOGUT	37.0363	29.8214	206	1.4	0.23	D	C	ZD	D-1
33	3111	KİRİKHAN TOPBOGAZI	36,00	36,30164	191	1.6	1.06	D	C	ZD	D-2
34	3112	İSKENDERUN	36,58801	36,14766	233	6.6	0.2	D	C	ZD	C-2
35	3113	İSKENDERUN	36,57752	36,15496	221	0.8	0.67	D	C	ZD	C-3
36	3114	İSKENDERUN	36,56704	36,15135	215	3.2	1.35	D	C	ZD	C-3
37	3115	İSKENDERUN	36,54634	36,16459	414	2.5	1.1	C	B	ZC	D-2
38	3116	İSKENDERUN	36,61618	36,20661	870	1.6	0.23	B	B	ZB	C-1
39	3117	İSKENDERUN	36,55712	36,17471	597	2.2	0.24	C	B	ZC	C-1

TABLE 1 CONTINUEE

Station Code	Station Name	Lat (°N)	Lon (°E)	V _{S30} (m/s)	H/V peak amplitude	Predominant period (sn)	[1]	[2]	[3]	[4]
40	3119 İSKENDERUN	36,57527	36,16811	374	3.2	0.2	C	B	ZC	C-1
41	3120 İSKENDERUN	36,58924	36,20568	455	3.1	0.26	C	B	ZC	C-1
42	3121 İSKENDERUN	36,66408	36,21825	271	8.5	0.43	D	C	ZD	C-3
43	3122 YAYLADAG	36,0343	36,107	1011	2.1	0.19	B	A	ZB	B
44	3124 ANTAKYA	36,2387	36,1722	283	4.1	0.81	D	C	ZD	D-1
45	3125 ANTAKYA	36,23808	36,13264	448	5.2	1.06	C	B	ZC	D-1
46	3126 ANTAKYA	36,2202	36,1375	350	2.06	0.16	D	C	ZD	C-3
47	3127 ANTAKYA	36,21	36,1353	404	3.6	0.12	C	B	ZC	B
48	3128 ANTAKYA	36,2056	36,1471	329	2.4	0.3	D	C	ZD	D-1
49	3129 ANTAKYA	36,19117	36,1343	447	2.06	0.07	C	B	ZC	C-1
50	3130 ANTAKYA	36,1792	36,145	447	3.2	0.07	C	B	ZC	B
51	3131 ANTAKYA	36,19121	36,16328	567	4.3	0.59	C	B	ZC	C-3
52	3132 ANTAKYA	36,20673	36,17159	377	2.49	0.29	C	B	ZC	C-1
53	3133 ANTAKYA	36,2432	36,5736	377	4.6	1.19	C	B	ZC	D-2
54	3134 DORTYOL	36,82763	36,20485	374	1.8	1.04	C	B	ZC	D-2
55	3135 ULUCINAR	36,40886	35,8831	460	2.9	0.1	C	B	ZC	C-2
56	3143 HASSA AKBEZ	36,84891	36,55714	444	2.2	1.42	C	B	ZC	D-2
57	3144 HASSA HACILAR	36,75746	36,48601	485	2.2	1.1	C	B	ZC	D-2
58	3145 KIRIKHAN BALARMUDU	36,64537	36,40642	533	1.68	0.47	C	B	ZC	C-2
59	3302 AKKUYU	36.1613	33.57584	1007	2.2	0.41	B	A	ZB	C-2
60	3303 CAMLIYAYLA	37.1659	34.60043	612	2.09	0.25	C	B	ZC	C-1
61	3304 SILIFKE	36.38226	33.93664	297	2.2	1.47	D	C	ZD	E-2
62	3305 TARSUZ	39.92142	34.89897	362	3.7	0.24	C	B	ZC	C-1
63	3306 MUT	36.64169	33.43956	490	4.7	0.1	C	B	ZC	B
64	3307 ANAMUR	36.08189	32.84224	855	1.2	0.1	B	A	ZB	B
65	8004 KADIRLI	37.37992	36.09757	426	2.2	0.13	C	B	ZC	B

Fig. 8. S-wave, V_{S30}, distribution in the Akdeniz region

The sites were classified in accordance with NEHRP Provisions [1], Eurocode-8 [2], TBDY [3] and Rodrigez and Marez (2001), (Table 1). The NEHRP Provisions suggest six site classes such as A, B, C, D, E, and F for the recognition of site conditions. 1 station is classified as class A, 7 stations as B and 38 stations as C and 19 stations to be class D. According to Eurocode-8 [2], 6 stations correspond to class A, 39 stations B, and 20 stations D which are similar to NEHRP provision. The classes of C, B, and A in NEHRP correspond to classes of B, A, and C in Eurocode-8 system since the boundary values of

class C in the NEHRP system coincide with the boundary values of class B in Eurocode-8, the boundary values of class B come up to the boundary values of class A and the boundary values of class D match with the boundary values of class C. The soil classes in the NEHRP system correspond to that of TBDY-2018 as seen in Table 1. According to [4] soil classifications, 8 stations are classified as A, 17 stations B, 8 stations C-1, 13 stations C-2, 5 stations C-3, 11 stations D-1, 1 station D-2, 1 station D-3, 1 station E and 1 station is undistinguished (Figure 9, Figure 10, Figure 11, Figure 12).

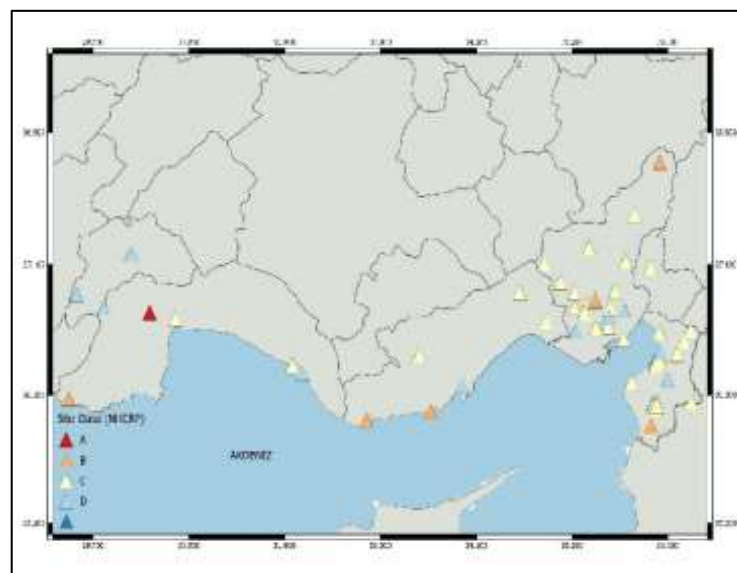


Fig. 9. NEHRP classification of the Akdeniz region

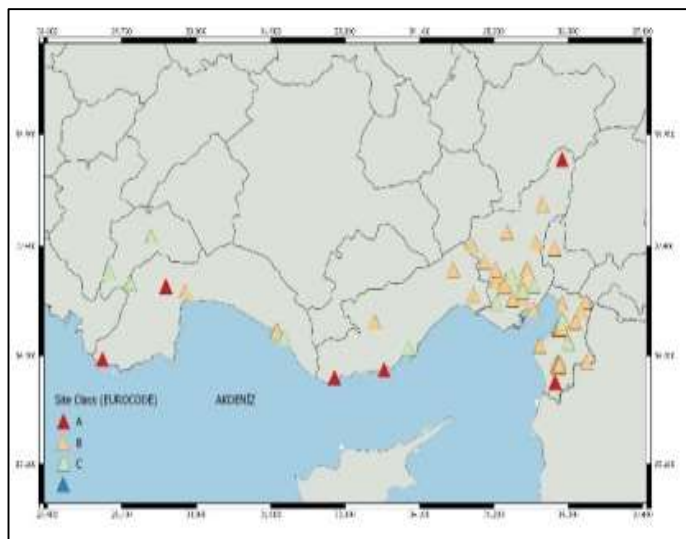


Fig. 10. Eurocode-8 classification of the Akdeniz region

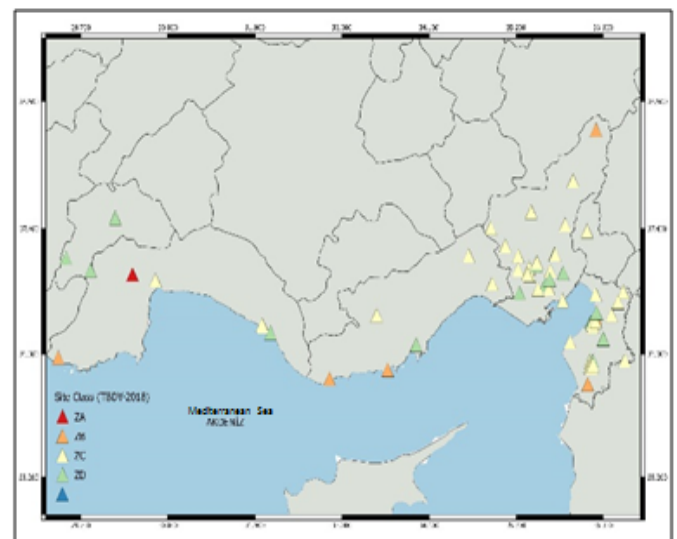


Fig. 11. TBDY classification of the Akdeniz region

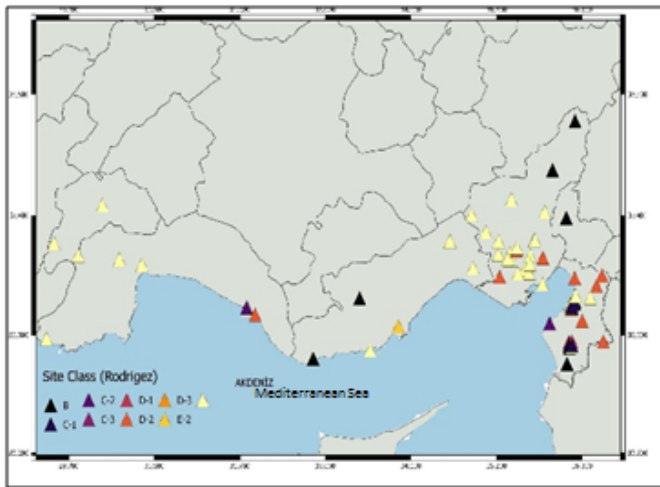


Fig. 12. Rodriguez and Marez classification of the Akdeniz region

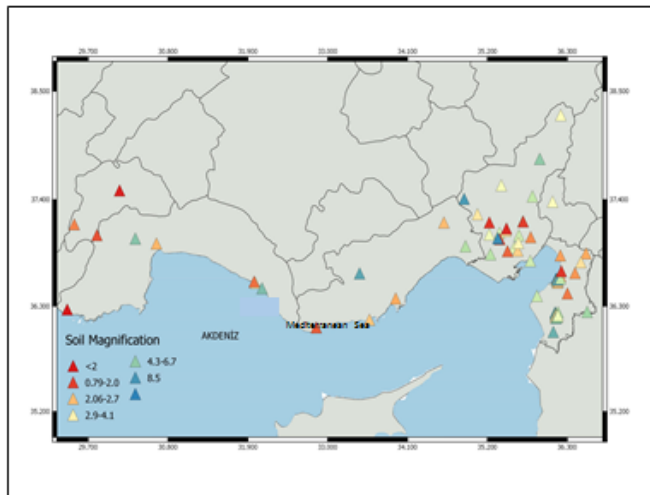


Fig. 13. Soil magnification of the Akdeniz region

B. Site amplification properties of Akdeniz region

Amplification ratios (H/V) and predominant periods were determined at 65 stations. Soil amplification and predominant periods were interpreted by Geopsy2004 software. The H/V ratios were determined between 0.79-8.5. The small magnification values (0.79-2.3) are generally observed on the stations located on the mountains, and higher values (2.3-8.5) were found in plain areas (Figure 13).

IV. DISCUSSION AND CONCLUSION

The V_{s30} values range from 191 to 1822m/s which are similar to the velocities determined by [29] in the Hatay province of this region. The lower velocities are generally determined on the plain areas. The lowest V_{s30} value was determined at 0117 coded Topbogazi station and the highest value at 707 coded Korkuteli station. The Akdeniz region was classified according to NEHRP Pro-

visions [1], Eurocode-8 [2], Turkish Building Earthquake Regulations [3] and [4]. According to NEHRP classification system the soil class of 38 stations is C and 19 stations is D indicating weak soil types. In this system only 1 station is determined as class A indicating strong soil and 7 stations indicating moderately hard soil. The soil classes in the NEHRP system correspond to that of TBDY-2018. According to Eurocode-8, 6 stations correspond to class A, 39 stations B, and 20 stations D which are similar to NEHRP provision. According to [4] soil classification; 8 stations are classified as A, 17 stations B, 8 stations C-1, 13 stations C-2, 5 stations C-3, 11 stations D-1, 1 station D-2, 1 station D-3, 1 station E and 1 station is undistinguished. The soil amplification values were determined between 0.7 and 8.5 sec. The lowest amplification value is observed at 111 coded Seyhan station and the highest at 3121 coded Iskenderun station. The higher amplification values are generally obtained on the plain areas. These values are in good agreement with the values determined by [29]. The max and the min predominant periods were determined as 0.07sec at 3129 and 3130 coded stations and 1.47 sec at 101, 707 and 3304 coded stations. Predominant periods of values generally increase with decreasing V_{s30} velocities.

The results determined in this study formed the basis of the site properties of the Akdeniz region. However; more studies are necessary to define the detailed site characteristics of the region.

REFERENCES

- [1] Building Seismic Safety Council, "NEHRP recommended provisions for seismic regulations for new buildings and other structures part 1: Provisions," National institute of building sciences, Washington, DC, WA, Tech. Rep., 2003.
- [2] P. Bisch, E. Carvalho, H. Degee, P. Fajfar, M. Fardis, P. Franchin, M. Kreslin, A. Pecker, P. Pinto, A. Plumier, H. Somja, and G. Tsionis, "Eurocode 8: Seismic design of buildings worked examples," European Commission, Brussels, Belgium, Tech. Rep., 2012.
- [3] TBDY. (2018) Turkey building earthquake regulation. [Online]. Available: <https://bit.ly/2Dxgafu>
- [4] A. Rodriguez-Marek, J. D. Bray, and N. A. Abrahamson, "An empirical geotechnical seismic site response procedure," *Earthquake Spectra*, vol. 17, no. 1, pp. 65-87, 2001. doi: <https://doi.org/10.1193/1.1586167>
- [5] B. Kemal, E. Mustafa, M. Cihat, and E. Zahi, "Seismic from the past to the present the activity and what to do in the light of the international conference eval-

- uation,” *Turkish Engineer News*, vol. 1, no. 423, pp. 51–53, 2003.
- [6] U. Tari, O. Tüysüz, Ş. Can Genç, C. İmren, B. A. Blackwell, N. Lom, Ö. Tekeşin, S. Üsküplü, L. Erel, S. Altıok *et al.*, “The geology and morphology of the Antakya Graben between the Amik Triple Junction and the Cyprus Arc,” *Geodinamica Acta*, vol. 26, no. 1-2, pp. 27–55, 2013. doi: <https://doi.org/10.1080/09853111.2013.858962>
- [7] R. C. Ates and N. Bayülke, “The 19 August 1976 Denizli, Turkey, earthquake: Evaluation of the strong motion accelerograph record,” *Bulletin of the Seismological Society of America*, vol. 72, no. 5, pp. 1635–1649, 1982.
- [8] N. N. Ambraseys, E. Durukal, and M. Free, “Re-evaluation of strong-motion data from Turkey,” Imperial College of Science, Technology and Medicine, London, UK, ESEE Research Report, No. 93/2, 1993.
- [9] O. Aydan and Z. Hasgür, “The characteristics of acceleration waves of Turkish earthquakes,” In *Proceedings of the 4th National Conference on Earthquake Engineering*, Ankara, Turkey, 1997.
- [10] M. Celebi, S. Akkar, U. Gulerce, A. Sanli, H. Bundoock, and A. Salkin, “Main shock and aftershock records of the 1999 Izmit and Duzce, Turkey earthquakes,” U.S. Geological Survey, Reston, VA, Tech. Rep., 2001.
- [11] E. Durukal, Y. Alpay, T. Biro, A. Mert, and M. Erdik, “Analysis of strong motion data of the 1995 Dinar, turkey earthquake, second Japan–Turkey workshop: Earthquake disaster prevention research in Turkey,” Istanbul Technical University, Istanbul, Turkey, Tech. Rep., 1998.
- [12] M. Erdik and E. Durukal, “1999 Kocaeli and Düzce, Turkey earthquakes: Strong ground motion,” In *XV ICSMGE TC4 Satellite Conference on Lessons Learned from Recent Strong Earthquakes*, Istanbul, Turkey, 1999.
- [13] M. Zaré and P.-Y. Bard, “Strong motion dataset of Turkey: Data processing and site classification,” *Soil Dynamics and Earthquake Engineering*, vol. 22, no. 8, pp. 703–718, 2002. doi: [https://doi.org/10.1016/s0267-7261\(02\)00028-3](https://doi.org/10.1016/s0267-7261(02)00028-3)
- [14] S. Ozalaybey, M. Ergin, M. Aktar, C. Tapirdamaz, F. Biçmen, and A. Yoruk, “The 1999 Izmit earthquake sequence in Turkey: Seismological and tectonic aspects,” *Bulletin of the Seismological Society of America*, vol. 92, no. 1, pp. 376–386, 2002. doi: <https://doi.org/10.1785/0120000838>
- [15] E. M. Rathje, K. H. Stokoe, and B. Rosenblad, “Strong motion station characterization and site effects during the 1999 earthquakes in Turkey,” *Earthquake Spectra*, vol. 19, no. 3, pp. 653–675, 2003. doi: <https://doi.org/10.1193/1.1596212>
- [16] M. Ergin, M. Aktar, and H. Eyidogan, “Present-day seismicity and seismotectonics of the Cilician Basin: Eastern Mediterranean Region of Turkey,” *Bulletin of the Seismological Society of America*, vol. 94, no. 3, pp. 930–939, 2004. doi: <https://doi.org/10.1785/0120020153>
- [17] D. Kalafat, Y. Güneş, M. Kara, P. Deniz, K. Kekovalı, H. Kuleli, L. Gülen, M. Yılmaz, and N. Özel, “A revised and extended earthquake catalogue for Turkey since 1900 ($m \geq 4.0$),” mthesis, Bogaziçi University, Istanbul, Turkey, 2007.
- [18] Ö. Erdoğan, “Main seismological features of recently compiled Turkish strong motion database,” Middle East Technical University, Ankara, Turkey, Tech. Rep., 2008.
- [19] M. A. Sandkkaya, “Site classification of national strong-motion recording sites,” mthesis, Civil Engineering Department, Middle East Technical University, Ankara, Turkey, 2008.
- [20] M. A. Sandikkaya, M. T. Yılmaz, B. S. Bakır, and Ö. Yılmaz, “Site classification of Turkish national strong-motion stations,” *Journal of Seismology*, vol. 14, no. 3, pp. 543–563, 2010. doi: <https://doi.org/10.1007/s10950-009-9182-y>
- [21] E. Kalkan and P. Gulkan, “Site-dependent spectra derived from ground motion records in Turkey,” *Earthquake Spectra*, vol. 20, no. 4, pp. 1111–1138, 2004. doi: <https://doi.org/10.1193/1.1812555>
- [22] R. Ulusay, E. Tuncay, H. Sonmez, and C. Gokceoglu, “An attenuation relationship based on turkish strong motion data and iso-acceleration map of Turkey,” *Engineering Geology*, vol. 74, no. 3-4, pp. 265–291, 2004. doi: <https://doi.org/10.1016/j.enggeo.2004.04.002>
- [23] Ö. Yılmaz, E. Savaşkan, B. Bakır, M. Yılmaz, M. Eser, S. Akkar, B. Tüzel, Y. İravul, Ö. Özmen, and Z. Denizlioğlu, “Shallow seismic and geotechnical site surveys at the Turkish national grid for strong-motion seismograph stations,” In *Proceedings 14th World Conference on Earthquake Engineering*, Beijing, China, 2008.
- [24] P. Gulkan, U. Ceken, Z. Colakoglu, T. Ugras, T. Kuru, A. Apak, J. Anderson, H. Sucuoglu, M. Celebi, D. Akkar *et al.*, “Enhancement of the national strong-motion network in Turkey,” *Seismological Research Letters*, vol. 78, no. 4, pp. 429–438, 2007.

- [25] S. Över, A. Büyüksaraç, Ö. Bekta, and A. Filazi, "Assessment of potential seismic hazard and site effect in Antakya (Hatay Province), SE Turkey," *Environmental Earth Sciences*, vol. 62, no. 2, pp. 313–326, 2011. doi: <https://doi.org/10.1007/s12665-010-0525-3>
- [26] H. Korkmaz, "Between antiquity soil properties and earthquake effect," *Journal of Relationships, Geographical Sciences*, vol. 4, no. 2, pp. 49–66, 2006.
- [27] S. Ş. Horoz, "Analysis of the seismicity of the region between adana-antakya-kahramanmara with the parameter 'b' kahraman and risk analysis." Cumhuriyet University, Sivas, Turkey, Tech. Rep., 2008.
- [28] O. Polat and U. Çeken, "Investigation of the local soil effects at the new strong-motion array (MAT-Net) in Hatay-K. Maras Region, Turkey," In *AGU Fall Meeting*, San Francisco, CA, 2014.
- [29] Ö. T. Özmen, H. Yamanaka, M. A. Alkan, U. Çeken, T. Öztürk, and A. Sezen, "Microtremor array measurements for shallow S-wave profiles at strong-motion stations in Hatay and Kahramanmaraş Provinces, Southern Turkey," *Bulletin of the Seismological Society of America*, vol. 107, no. 1, pp. 445–455, 2016. doi: <https://doi.org/10.1785/0120160218>
- [30] S. V. Aditya, M. Duraiselvam, K. Parthiban, and V. Bagade, "Laser surface texturing of nickel superalloy to improve adhesion bond strength of thermal barrier coating," *International Journal of Applied and Physical Sciences*, vol. 3, no. 3, pp. 85–92, 2017. doi: <https://doi.org/10.20469/ijaps.3.50005-3>
- [31] T. S. Irmak and M. F. Özer, "23rd February, 1990 cyprus earthquake welding mechanism," *Earthquake Research Bulletin*, vol. 80, pp. 109–134, 1999.
- [32] N. Febryanti and D. Gunawan, "PAPR reduction in OFDM system with wavelet transformation and partial transmit sequence technique," *Journal of Advances in Technology and Engineering Studies*, vol. 3, no. 1, pp. 1–5, 2017. doi: <https://doi.org/10.20474/jater-3.1.1>
- [33] C. Park, R. Miller, and J. Xia, "Multi-channel analysis of surface waves (MASW)," *Geophysics*, vol. 64, no. 3, pp. 800–808, 1999. doi: <https://doi.org/10.1190/1.1444590>
- [34] J. Xia, R. D. Miller, and C. B. Park, "Estimation of near-surface shear-wave velocity by inversion of rayleigh waves," *Geophysics*, vol. 64, no. 3, pp. 691–700, 1999. doi: <https://doi.org/10.1190/1.1444578>